5. Tomalia, D. A., Naylor, A. M. & Goddard, W. A. *Angew. Chem. int. Edn. engl.* **29**, 138–175 (1990).
6. Tomalia, D. A. *Aldrichim. Acta* **26**, 91–101 (1993).
7. Achar, S. & Puddephatt, R. J. *Angew. Chem. int. Edn. engl.* **33**, 1493–1495 (1994).
8. Serroni, S. *et al. Angew. Chem. int. Edn. engl.* **31**, 1493–1495 (1992).
9. Moulines, F., Gloaguen, B. & Astruc, D. *Angew. Chem. int. Edn. engl.* **31**, 458–460 (1992).
10. Newkome, G. R. *et al. J. chem. Soc., chem. Commun.* 925–927 (1993).
11. Liao, Y-H. & Moss, J. R. *J. chem. Soc., chem. Commun.* 1774–1777 (1993).
12. van de Kuil, L. A. *et al. Recl Trav. chim. Pays-Bas* **113**, 267–277 (1994).
13. van der Made, A. W. & van Leeuwen, P. W. N. M. *J. chem. Soc., chem. Commun.* 1400–1401 (1992).
14. van der Made, A. W., van Leeuwen, P. W. N. M., de Wilde, J. C. & Brandes, R. A. C. *Adv. Mater.* **5**, 466–468 (1993).
15. Seyferth, D., Son, D. Y., Rheingold, A. L. & Ostrander, R. L. *Organometallics* **13**, 2682-2690 (1994).
16. Eckert, H. & Forster, B. *Angew. Chem. int. Edn. engl.* **99**, 922–923 (1987).
17. Grove, D. M., van Koten, G., Ubbels, H. J. C., Zoet, R. & Spek, A. L. *Organometallics* **3**, 1003–1009 (1984).
18. Grove, D. M. *et al. Inorg. Chem.* **27**, 2466–2473 (1988).
19. Grove, D. M., van Koten, G. & Verschuuren, A. H. M. *J. Molec. Catal.* **45**, 169–174 (1988).
20. Grove, D. M., Verschuuren, A. H. M., van Koten, G. & van Beek, J. A. M. *J. organomet. Chem.* **372**, C1–C6 (1989).

ACKNOWLEDGEMENT. We thank J. Thomas-Oates for acquiring the FAB mass spectra of **1**.

Climate correlations between Greenland and Antarctica during the past 100,000 years

Michael Bender*, Todd Sowers†, Mary-Lynn Dickson*, Joseph Orchardo*, Pieter Grootes‡, Paul A. Mayewski§ & Debra A. Meese‖

* Graduate School of Oceanography, University of Rhode Island, Kingston, Rhode Island 02881, USA
† Lamont-Doherty Earth Observatory, Palisades, New York 10964, USA
‡ Department of Geological Sciences and Quaternary Research Center, University of Washington, Seattle, Washington 98105, USA
§ Glacier Research Group, Institute for the Study of Earth, Oceans and Space, University of New Hampshire, Durham, New Hampshire 03824, USA
‖ Cold Regions of Research and Engineering Laboratory, Hanover, New Hampshire 03755, USA

THE ice cores recovered from central Greenland by the GRIP[1,2] and GISP2[3] projects record 22 interstadial (warm) events during the part of the last glaciation spanning 20–105 kyr before present. The ice core from Vostok, east Antarctica, records nine interstadials during this period[4,5]. Here we explore links between Greenland and Antarctic climate during the last glaciation using a high-resolution chronology derived by correlating oxygen isotope data for trapped O_2 in the GISP2 and Vostok cores. We find that interstadials occurred in east Antarctica whenever those in Greenland lasted longer than 2,000 years. Our results suggest that partial deglaciation and changes in ocean circulation are partly responsible for the climate teleconnection between Greenland and Antarctica. Ice older than 115 kyr in the GISP2 core shows rapid variations in the $\delta^{18}O$ of O_2 that have no counterpart in the Vostok record. The age–depth relationship, and thus the climate record, in this part of the GISP2, core appears to be significantly disturbed.

The oxygen isotope ratio ($\delta^{18}O$) of O_2 in the modern atmosphere ($\delta^{18}O_{atm}$) is ~23.5‰ heavier than mean ocean water[6], mainly due to fractionation of the oxygen isotopes during photosynthesis, respiration and hydrological processes[7–9]. (See Fig. 1 legend for a definition of $\delta^{18}O$). The $\delta^{18}O$ of sea water ($\delta^{18}O_{sw}$) has varied with fluctuations in the volume of continental ice[10]. During the past 135 kyr, $\delta^{18}O_{atm}$ has followed $\delta^{18}O_{sw}$ variations because photosynthesis transmits variations in $\delta^{18}O_{sw}$ to O_2 in air[11,12]. Although $\delta^{18}O$ of O_2 varies with time, it is constant throughout the atmosphere at any one time because the turnover time of O_2 ($\sim 1.2 \times 10^3$ yr)[9] is much longer than the mixing time of the atmosphere (~1 yr). Hence $\delta^{18}O$ of O_2 can be used to intercorrelate ice cores, and to correlate ice cores with the deep-sea sediment oxygen-isotope stratigraphy[11,12].

Sowers *et al.*[11] measured $\delta^{18}O_{atm}$ in the Vostok ice core and used the results to establish a chronology for trapped gases in that ice core which is consistent with the SPECMAP chronology (Fig. 1). We present a new record of $\delta^{18}O_{atm}$ from the GISP2 core (based on the analysis of 201 samples between 100 and 3,050 m depth) and use the results to establish a chronology which is consistent with that of Vostok[11] as well as the deep-sea sediment record (Fig. 1). Because $\delta^{18}O_{atm}$ is relatively constant between 25 and 49 kyr ago, we consider the correlations between Vostok, SPECMAP and GISP2 to be inadequate during this period, and focus our discussion on ice which is older than 49 kyr.

We derive an age–depth relationship for the GISP2 core by correcting for the fact that gases are trapped 70–90 m below the surface, making the gas younger than the surrounding ice[13,14]. Our ice-core chronologies are not necessarily the most accurate, but they provide the most precise relative ages for comparing GISP2 and Vostok climate records with one another as well as with deep-sea records in the range 50–105 kyr. We estimate the uncertainty in relative ice ages at GISP2 and Vostok as <3 kyr, half of which comes from uncertainties in correlating gas records and half from uncertainties in differences between gas and ice ages at Vostok. We also note that our absolute chronology is in excellent agreement with that derived for the GRIP core by Dansgaard *et al.*[2] based on a flow model and assigned ages for two depths in the core.

In Fig. 1, we plot δD of Vostok ice (δD_{ice})[5,15] and $\delta^{18}O$ of GISP2 ice ($\delta^{18}O_{ice}$)[3] against SPECMAP age. The isotopic composition of hydrogen and oxygen in precipitation reflect condensation temperatures, with heavier values corresponding to warmer temperatures. There are 22 distinct interstadial events recorded in the GISP2 (and GRIP) record between 20 and 105 kyr ago (refs 1–3). These well documented events range in duration from ~0.4 to 12 kyr (from first warming to final cooling). Eight of the nine long (>2 kyr from glacial baseline to glacial baseline) interstadial events at GISP2 can be clearly recognized in the Vostok record as increases in δD of at least 15‰, corresponding to warmings of 2 °C or more[16,17]. The correlation of events 8 and 12 to Vostok events dated at 39 and 46 kyr is uncertain because the Vostok chronology is poorly defined in this period. Small warming events, largely buried in the noise at Vostok, may correspond to the shorter Greenland interstadials, but these events cannot be intercorrelated with confidence.

The nature of the correlated long interstadial events differs between Greenland and Antarctica. In Greenland, interstadial events (from cold baseline to cold baseline) are characterized by very rapid warming, moderate cooling during the interstadial, and then very rapid cooling at its end. At Vostok, related events are characterized by slow warmings and slow coolings. Interstadial events 21 and 23 appear to coincide between GISP2 and Vostok, but we cannot say whether Greenland or Antarctica warmed first. Other events may be in phase or out of phase given present resolution. We are impressed by the observations that climate change is more rapid, and events more numerous, in Greenland than in Antarctica. We infer that, during the last glacial period, interstadials began in the Northern Hemisphere and subsequently spread to Antarctica if they lasted long enough. However, this inference cannot yet be proven. Furthermore, the nature of interstadial forcing and response may vary from one event to the next.

A number of factors may be responsible for the interstadial events observed in Greenland and Antarctica, and their approximate synchrony. Insolation is the first factor, especially because orbital frequencies have been identified in both the Vostok and Greenland temperature records[2,18]. Interstadials 21 and 23 fall within marine isotope substages 5a and 5c, respectively, and may be linked (perhaps with a 3–5 kyr delay) to the maxima in summertime insolation at 60° N which occurred about 84 and 105 kyr ago[15]. Long interstadial events 8, 12, 14, and 16+17 occur during a period of moderate summertime insolation at 60° N which lasted from 35 to 59 kyr and may have favoured these episodes of warmer climate.

A second factor is sea level (or continental ice volume), which is associated with much of the variability observed in the Vostok temperature record[19]. Changes in sea level and ice volume could directly affect climate by destabilizing ice shelves, by changing albedo, and by causing changes in the production rates of warm, salty water in marginal basins (and hence oceanic meridional heat fluxes)[20]. There is a remarkably strong connection between long interstadial events in Greenland and minima in $\delta^{18}O$ of benthic foraminifera in equatorial Pacific core V19-30 (Fig. 1), as previously implied by Bond *et al.*[21].

Third, North Atlantic Deep Water (NADW) production leads to a large flux of heat from oceans to atmosphere in the subpolar north Atlantic[22]. There is ample evidence that lower NADW production slowed or ceased during much of the last glacial period[23,24]. Bond *et al.*[21] and Keigwin and Jones[25] have invoked the startup of NADW production as the immediate cause of rapid warming associated with interstadial events in Greenland. North Atlantic Deep Water is an important source of warm, salty water to the Antarctic circumpolar current; it therefore contributes to oceanic heating of the atmosphere between 60° and 75 °S (refs 26–28). Evidence for a link between NADW production and interstadial events at Vostok comes from recent work of Keigwin and Jones[25]. They observed that changes in sedimentation in the western north Atlantic, thought to be induced by NADW formation, coincide with Vostok interstadials at ~50 kyr (corresponding to Greenland interstadial event 14), 55–60 kyr (events 16 and 17), 68 kyr (event 19), 72 kyr (event 20) and 80 kyr (event 21). Increased production of NADW from its low glacial values could have warmed Antarctica in two ways. (1) By increasing the heat released from the ocean to air[26–29] causing a reduction in the maximum extent of winter sea ice which is further amplified by a reduced albedo, and (perhaps more likely) (2) by moving belts of Antarctic climate southwards and thereby increasing poleward heat transport through the atmosphere[30]. This hypothesis is supported by Charles and Fairbanks' deep-water $\delta^{13}C$ record[23] from the Southern Ocean which suggests that the formation of NADW increased during the last deglaciation. On the other hand, modelling studies suggest that enhanced NADW production would actually cool the Southern Hemisphere by displacing warm intermediate waters towards the north[31,32]. This latter work suggests that interstadial events in Greenland and Antarctica should be out of phase when they are unaccompanied by large variations in continental ice volume and atmospheric CO_2. Given age uncertainties, we cannot exclude this possibility for related interstadial events 8, 12, 14, 16, 19 or 20.

The fourth event forcing factor is the greenhouse effect. During interstadial events, CH_4 concentrations rise by ≥ 100 parts per billion (by volume)[33,34], an increase which could cause temperatures at Vostok to rise by as much as 0.3 °C (~10% of the observed increase)[33]. The link between CO_2 and Vostok temperatures is weaker. Only between 55 and 65 kyr ago (during interstadial events 16 and 17) does CO_2 increase coherently with Vostok temperature[35]. The increase is ~25 parts per million (by volume), which could correspond to a temperature rise of up to 0.6 °C at Vostok, or ~20% of the total interstadial temperature rise.

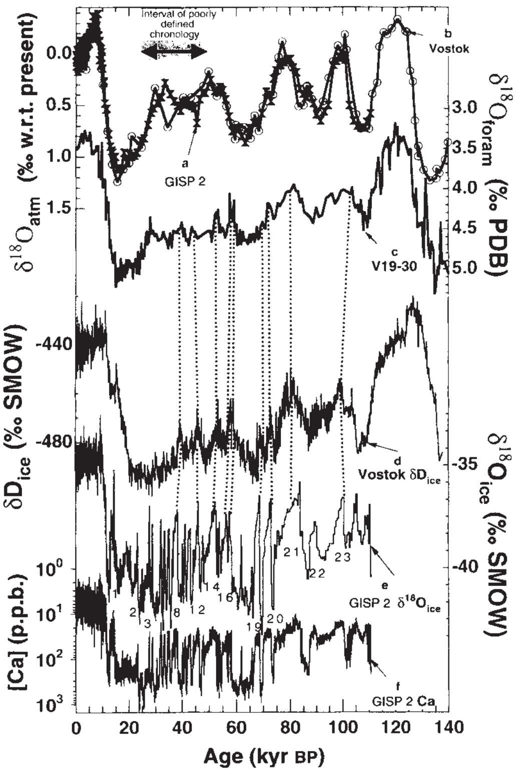

FIG. 1 Greenland and Antarctic climate records covering the last glacial–interglacial cycle. For the timescale (kyr before present, BP), we adopt the layer-counting chronology of Meese *et al.*[45] and Alley *et al.*[46] for GISP2 to 2,250 m depth; we derive a gas age–depth relation for the GISP2 core between 2,250 and 2,800 m by correlating the GISP2 $\delta^{18}O_{atm}$ record into the Vostok $\delta^{18}O_{atm}$ record of Sowers *et al.*[11] between 37.9 and 110 kyr. a, b, $\delta^{18}O_{atm}$ records from GISP2 (a) and Vostok (b) ice cores. Note the interval over which the Vostok timescale is poorly defined (25–49 kyr). c, The benthic $\delta^{18}O_{foram}$ record from deep-sea sediment core V19-30 (3° 21′ S, 83° 21′ W, 3,091 m; *Uvigerina senticosa*)[47] showing continental ice volume variations. d, Vostok isotope temperature (δD_{ice}) with dashed lines tying the interstadial events at Vostok with the longer Dansgaard–Oeschger events in GISP2 ($\delta^{18}O_{ice}$) (e). Note the numbered interstadial events below the GISP2 record as identified in ref. 2. Also shown (f) is the [Ca] data from GISP2 on an inverted log scale. Our results indicate that for each Greenland interstadial event lasting >2 kyr, there is a corresponding warm event over Antarctica. Warm interstadial events may be related to local minima in the $\delta^{18}O_{foram}$ record from V19-30 indicative of high sea-level stands. Points on the ice age–depth curve for GISP2 lie as follows: 2,450 m, 52.4 kyr; 2,500 m, 57.5 kyr; 2,550 m, 63.8 kyr; 2,589 m, 69.5 kyr; 2,628 m, 75.6 kyr; 2,667 m, 82.2 kyr; 2,693 m, 87.6 kyr; 2,719 m, 93.8 kyr; 2,745 m, 100.1 kyr; 2,784 m, 107.4 kyr; and 2,808 m, 111.0 kyr. ($\delta^{18}O = \{[(^{18}O/^{16}O)_{sample}/(^{18}O/^{16}O)_{standard}] - 1\}$ per mil. The standard used is indicated on the figure: 'present', present-day values; PDB, standard rock; SMOW, standard mean ocean water. Similarly, $\delta D = \{[(D/H)_{sample}/(D/H)_{standard}] - 1\}$ per mil.)

METHODS. GISP2 samples (201) were analysed for $\delta^{18}O$ of O_2 and the $\delta^{15}N$ of N_2 using the method of Sowers *et al.*[48]. We corrected the measured $\delta^{18}O$ of O_2 for gravitational fractionation using the measured $\delta^{15}N$ of N_2 in the following equation: $\delta^{18}O_{atm} = \delta^{18}O$ of $O_2 - 2(\delta^{15}N$ of $N_2)$. The standard deviation of $\delta^{18}O_{atm}$ values from the mean of replicates is ±0.04‰. The GISP2 $\delta^{18}O_{atm}$ record from 2,235.1 to 2,800 m depth was correlated into the Vostok $\delta^{18}O_{atm}$ record from Sowers *et al.*[11] between 37.9 and 110.0 kyr using an inverse correlation technique[49]. The final mapping function has three coefficients and yielded an r^2 value of 0.96. We then constructed an ice age–depth profile by correcting for differences between the ages of gas and ice based on the protocol developed by Sowers *et al.*[50]. The resulting ice age–depth profile for GISP2 differs from that based on layer counts below 2,400 m (50 kyr). At this point the two age models begin to diverge with increasing depth until they reach a maximum difference of 26 kyr at 2,800 m. The origin of the discrepancy is being investigated. It may reflect a combination of loss of annual layers due to thinning and errors in the absolute chronology to which the $\delta^{18}O_{atm}$ curve is referenced.

Fifth and finally, ice-sheet modelling by MacAyeal suggests that some interstadial events may be caused by the episodic rapid discharge of large volumes of ice from the Northern Hemisphere ice sheets[36,37]. Evidence of such discharge has been preserved in the Heinrich layers in North Atlantic ocean sediments[21,38–40]. These Heinrich events have been closely correlated with the sequence of interstadial episodes in the Greenland ice core.

The slow change of Vostok temperatures during interstadial events suggests that the heat flux associated with changes in ocean circulation, as well as glacioeustatic changes in sea level, are important in transferring warmings in Northern Hemisphere climates to the Antarctic continent. Responses to other possible forcings are probably either too small (for example, radiative forcing by greenhouse gases) or too slow to account for the magnitude and shape of interstadial temperature–time curves observed at Vostok. Changes in atmospheric circulation could certainly be important, and could even have initiated the interstadial events, but would have been associated with changes in sea level or ocean circulation. With respect to climate variations induced by changes in ocean circulation, the time constant for reaching a new thermal steady-state might be as long as the oceanic turnover time of ~1 kyr. In the absence of ice-sheet surges, the time constant for growing or melting continental ice sheets is ~10 kyr. Melting ice sheets could cause sea level to rise a few tens of metres over a few thousand years. Thus partial deglaciation could also account for the response times of Antarctic climates.

In Fig. 2, we plot $\delta^{18}O_{atm}$ and $\delta^{18}O_{ice}$ records from the GISP2 core against depth for the interval of core below 2,750 m. We also plot Vostok δD and $\delta^{18}O_{atm}$ against age according to the extended glaciological time scale (EGT) of Jouzel *et al.*[15] for the period from 100 to 220 kyr ago. It is immediately obvious from this figure that the GISP2 curve of $\delta^{18}O_{atm}$, so similar to Vostok above 2,790 m depth, is very different below 2,850 m depth. At Vostok, the depth interval containing ice deposited between 110 and 220 kyr ago is 1,600 to 2,500 m depth. This interval is 1,200–2,100 m above bedrock and therefore unlikely to have stratigraphic discontinuities. The lack of covariation in the $\delta^{18}O_{atm}$ records must, therefore, be due to disturbance in the GISP2 core below 2,790–2,850 m depth. Disturbance has, in fact, been observed in the fabric and stratigraphy of the GISP2 ice[41] in the lower part of the core.

One interpretation of the GISP2 $\delta^{18}O_{atm}$ record below 2,850 m is that ice in the deep part of the core is affected by variable thinning but represents a continuous section except for minor loss of some parts of the section due to boudinage. According to this interpretation, $\delta^{18}O_{atm}$ minima at 2,846, 2,956 and 2,980 m depth can be correlated with minima at Vostok dated at 125, 180 and 210 kyr ago with the EGT chronology. The deepest $\delta^{18}O_{atm}$ minima in GISP2, at 2,998 and 3,002 m depth, are not found in the part of the Vostok core studied to date (back to 240 kyr) but might be correlative with the seawater $\delta^{18}O$ minima dated at 240 and perhaps 290 kyr ago in the SPECMAP timescale[42].

Such a chronology for GISP2 is extremely unlikely to be correct, for the following reasons. First, it requires that there be much more high-frequency variability in the $\delta^{18}O_{atm}$–time curve between 130–240 kyr than between 0–130 kyr. It also requires that this variability be absent from the Vostok record for the correlative period (age >130 kyr) because of a fortuitous choice of sampling depths in that core. Second, the above chronology requires that, between 175 and 185 kyr (corresponding to 2,950–2,960 m depth in GISP2), and during marine isotope stage 8 (corresponding to ~3,000 m depth in GISP2), Greenland temperatures be warmer than Holocene values, and that Ca concentrations reflect low interglacial values (indicating relatively wet climates and weak poleward atmospheric transport). Such conditions are not likely to have prevailed in Greenland throughout these periods when climates elsewhere were glacial[15,43]. Third, the above chronology for GISP2 implies that Greenland temperatures during most of marine isotope stage 7 were warmer than Holocene and as warm as during substage 5e. This is possible but suspicious nonetheless: during stage 7 North Atlantic sea surface temperatures were lower, ice volume (as indicated by $\delta^{18}O$ of foraminifera) was greater, and Vostok temperatures were colder than during the Eemian[29].

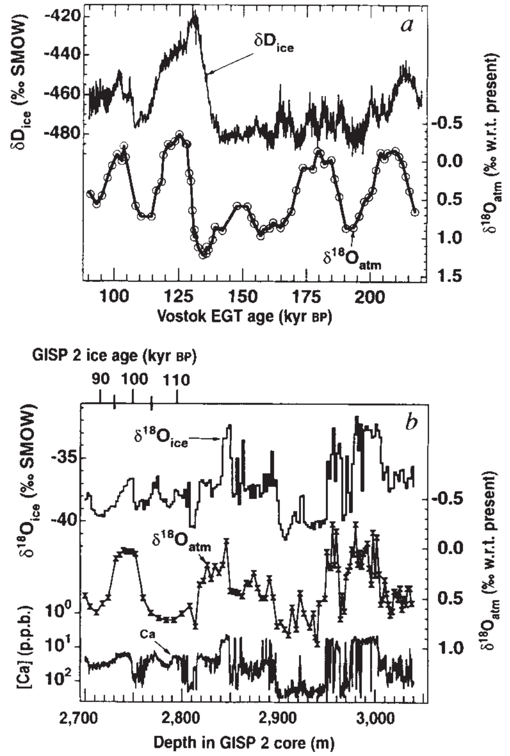

FIG. 2 *a*, δD of ice in the Vostok core for 90–240 kyr BP according to the EGT chronology[16]. Also shown in this panel is the Vostok $\delta^{18}O_{atm}$ record over the same time period showing smooth variations throughout. *b*, GISP2 $\delta^{18}O_{ice}$, $\delta^{18}O_{atm}$ and [Ca] records covering the bottom 350 m of the core. Of interest is the switch from smoothly varying $\delta^{18}O_{atm}$ above 2,800 m depth (100 kyr) to extreme $\delta^{18}O_{atm}$ variations below 2,800 m depth. Note the clear disagreement between the GISP2 and Vostok $\delta^{18}O_{atm}$ records in these two plots which we interpret as signifying discontinuities in the GISP2 core.

An alternative explanation for the $\delta^{18}O_{atm}$ record in the deep part of the GISP2 core is that it reflects more significant disturbance of the original stratigraphy. This could happen in two ways. First, the section could still be ordered correctly in terms of age but could be highly condensed by extensive loss of ice due to thinning and boudinage. In this case, the ages given above would be minimum ages. Ca concentrations <10 p.p.b. and $\delta^{18}O_{ice}$ values >−34‰ indicate interglacial conditions; the deep part of the core could contain five or more interglacial periods and be well over 400 kyr old. Thus one could, for example, correlate GISP2 $\delta^{18}O_{atm}$ minima at 2,846 and 2,956 m depth with 125- and 210-kyr minima at Vostok, and GISP2 $\delta^{18}O_{atm}$ minima at 2,980 and 2,998–3,002 m depth with $\delta^{18}O_{sw}$ minima dated at 325 and 405 kyr in the SPECMAP timescale. The coldest part of stage 6, corresponding to the 180-kyr $\delta^{18}O_{atm}$ minimum at Vostok, and other parts of the climate record would be missing at GISP2 according to this scheme. Second, flow may have caused ice of different ages to be intermixed as a result of folding and/or intrusion[41]. In either case, rapid changes with depth in climate proxies could signify either rapid climate changes or disturbances in the age–depth relationship.

We note that the heaviest $\delta^{18}O_{atm}$ value observed below 2,750 m depth is ~±0.9‰. Comparison with the Vostok profile shows that ice of age 130–140 kyr by the EGT chronology (corresponding to the coldest part of marine isotope stage 6) is therefore missing from GISP2, at least as sampled at 2–4 m depth increments. We also note that interglacial ice below 2,800 m in the GISP2 core consistently has $\delta^{18}O_{atm} = -0.25 \pm 0.10‰$, [Ca] ~ 5 p.p.b. and $\delta^{18}O_{ice} = -32 \pm 0.5‰$. We speculate that such ice samples may all have the same age, perhaps Eemian (corresponding to marine isotope substage 5e). It is possible that most ice in the GISP2 core below 2,850 m depth is largely from the latter part of Termination 2 (the penultimate deglaciation, ~128–140 kyr BP) and substages 5e and 5d. Finally, comparison of our data with Vostok suggests that the ice is disturbed below 2,790 m but may largely be in correct stratigraphic order to 2,850 m depth. Thus, it may be that ice between 2,790 and 2,850 m depth corresponds to the latter part of the Eemian (substage 5e) and the subsequent cooling (5e/5d transition).

One of the most intriguing results to emerge from the recent study of the GRIP ice core was the rapid $\delta^{18}O_{ice}$ variations within the Eemian, which were interpreted as rapid changes to colder climates[1]. This conclusion has been questioned by Taylor *et al.*[41] on the grounds that the GRIP core, like GISP2, may be disturbed below 2,750 m (110 kyr BP). The GRIP core, drilled over the current ice divide, might have been subjected to less disturbance than GISP2 if the divide had remained at its present position. On the other hand, if the divide migrated, and Anandakrishnan *et al.*[44] have in fact argued that such migration is likely, then flow could have disturbed the GRIP stratigraphy just as we have observed at GISP2. The question of continuity of the "Eemian" and deeper sections of the GRIP ice core remains unresolved. However, this work demonstrates that continuity of the GRIP ice core below 2,750 m depth could be conclusively established by showing that $\delta^{18}O_{atm}$ varies as it does at Vostok. □

Received 13 June; accepted 1 November 1994.

1. GRIP Project Members *Nature* **364,** 203–207 (1993).
2. Dansgaard, W. *et al. Nature* **364,** 218–220 (1993).
3. Grootes, P. M., Stuiver, M., White, J. W. C., Johnsen, S. & Jouzel, J. *Nature* **366,** 552–554 (1993).
4. Lorius, C. *et al. Nature* **316,** 591–595 (1985).
5. Jouzel, J. *et al. Nature* **329,** 403–407 (1987).
6. Kroopnick, P. & Craig, H. *Science* **175,** 54–55 (1972).
7. Lane, G. A. & Dole, M. *Science* **123,** 574–576 (1956).
8. Dongmann, G. *Radiat. Envir. Biophys.* **11,** 219–225 (1974).
9. Bender, M. L., Sowers, T. A. & Labeyrie, L. *Globl Biogeochem. Cycles* **8,** 363–376 (1994).
10. Shackleton, N. J. & Opdyke, N. D. *Quat. Res.* **3,** 39–55 (1973).
11. Sowers, T. *et al. Paleoceanography* **8,** 737–766 (1993).
12. Sowers, T., Bender, M., Raynaud, D., Korotkevich, Y. S. & Orchardo, J. *Paleoceanography* **6,** 679–696 (1991).
13. Schwander, J. in *The Environmental Record in Glaciers and Ice Sheets* (eds Oeschger, H. & Langway, C. C.) 53–67 (Wiley, New York, 1989).
14. Barnola, J. M., Pimienta, P., Raynaud, D. & Korotkevich, Y. S. *Tellus* **43B,** 83–90 (1991).
15. Jouzel, J. *et al. Nature* **364,** 407–412 (1993).
16. Bender, M., Sowers, T. & Orchardo, J. (abstr.) *EOS* **43,** 78 (1993).
17. Jouzel, J., Lorius, C., Johnsen, J. & Grootes, P. *C.r. hebd. Seanc. Acad. Sci., Paris* **319,** 65–77 (1994).
18. Genthon, C. *et al. Nature* **329,** 414–418 (1987).
19. Lorius, C., Jouzel, J., Raynaud, D., Hansen, J. & Le Treut, H. *Nature* **347,** 139–145 (1990).
20. Lynch-Stieglitz, J., Fairbanks, R. G. & Charles, C. D. *Paleoceanography* **9,** 7–29 (1994).
21. Bond, G. *et al. Nature* **365,** 143–147 (1993).
22. Broecker, W. S. & Denton, G. H. *Geochim. cosmochim. Acta* **53,** 2465–2501 (1989).
23. Charles, C. D. & Fairbanks, R. G. *Nature* **35,** 416–419 (1992).
24. Oppo, D. W. & Fairbanks, R. G. *Paleoceanography* **5,** 277–288 (1990).
25. Keigwin, L. D. & Jones, G. A. *J. geophys. Res.* **99,** 12397–12410 (1994).
26. Martinson, D. in *Ice and the Climate System* (ed. Peltier, W. R.) 597–609 (Springer, Berlin, 1993).
27. Nakamura, N. & Oort, A. *J. geophys. Res.* **93,** 9510–9524 (1988).
28. Gordon, A. & Huber, B. *J. geophys. Res.* **95,** 11655–11672 (1990).
29. Imbrie, J. *et al. Paleoceanography* **7,** 701–738 (1992).
30. Peixoto, J. P. & Oort, A. H. *Physics of Climate* (American Inst. of Physics, New York, 1992).
31. Crowley, T. J. *Paleoceanography* **7,** 489–499 (1992).
32. Stocker, T. F., Wright, D. G. & Mysak, L. A. *J. Clim.* **5,** 773–797 (1992).
33. Chappellaz, J., Barnola, J.-M., Raynaud, D., Korotkevich, Y. S. & Lorius, C. *Nature* **345,** 127–131 (1990).
34. Chappellaz, J. *et al. Nature* **366,** 443–445 (1993).
35. Barnola, J. M., Raynaud, D., Korotkevich, Y. S. & Lorius, C. *Nature* **329,** 408–414 (1987).
36. MacAyeal, D. R. *Paleoceanography* **8,** 767–774 (1993).
37. MacAyeal, D. R. *Paleoceanography* **8,** 775–784 (1993).
38. Broecker, W., Bond, G., Klas, M., Clark, E. & McManus, J. *J. Clim. Dyn.* **6,** 265–273 (1992).
39. Heinrich, H. *Quat. Res.* **29,** 142–152 (1988).
40. Bond, G. *et al. Nature* **360,** 245–249 (1992).
41. Taylor, K. C. *et al. Nature* **366,** 549–552 (1993).
42. Martinson, D. G. *et al. Quat. Res.* **27,** 1–27 (1987).
43. Sancetta, C., Imbrie, J. & Kipp, N. *Quat. Res.* **3,** 110–116 (1973).
44. Anandakrishnan, S., Alley, R. B. & Waddington, E. D. *Geophys. Res. Lett.* **21,** 441–444 (1994).
45. Meese, D. *et al. Preliminary Depth-age Scale of the GISP2 Ice Core* (Spec. Rep. 94-1, Cold Regions Research and Engineering Lab., Hanover, New Hampshire, 1994).
46. Alley, R. B. *et al. Nature* **362,** 527–529 (1993).
47. Shackleton, N. J. & Pisias, N. G. in *The Carbon Cycle and Atmospheric CO2: Natural Variations Archean to Present* (eds Sundquist, E. T. & Broecker, W. S.) 303–317 (American Geophysical Union, Washington DC, 1985).
48. Sowers, S., Bender, M. & Raynaud, D. *J. geophys. Res.* **94,** 5137–5150 (1989).
49. Martinson, D. G., Menke, W. & Stoffa, P. *J. geophys. Res.* **87,** 4807–4818 (1982).
50. Sowers, T., Bender, M., Raynaud, D. & Korotkevich, Y. S. *J. geophys. Res.* **97,** 15683–15697 (1992).

ACKNOWLEDGEMENTS. We thank the following for their comments; R. Alley, K. Taylor, S. Johnsen, S. Paterson, J. Jouzel and J. Chappellaz; also J. Schwander, T. Stocker and their colleagues at the University of Berne. We happily acknowledge the contribution of M. Wumkes and his team of drillers, and the input of our colleagues in the GISP2 programme. Partial support for T.S. was provided by UCSIO. This work was supported by the US National Science Foundation.

The role of deep roots in the hydrological and carbon cycles of Amazonian forests and pastures

Daniel C. Nepstad*, Claudio R. de Carvalho†, Eric A. Davidson*, Peter H. Jipp*‡, Paul A. Lefebvre*, Gustavo H. Negreiros*, Elson D. da Silva†, Thomas A. Stone*, Susan E. Trumbore§ & Simone Vieira*

* Woods Hole Research Center, Woods Hole, Massachusetts 02543, USA

† EMBRAPA-CPATU, CP 48, Belém, Pará 66.001, Brazil

§ Department of Earth System Sciences, University of California, Irvine, California 92717, USA

DEFORESTATION and logging transform more forest in eastern and southern Amazonia than in any other region of the world[1–3]. This forest alteration affects regional hydrology[4–11] and the global carbon cycle[12–14], but current analyses of these effects neglect an important deep-soil link between the water and carbon cycles. Using rainfall data, satellite imagery and field studies, we estimate here that half of the closed forests of Brazilian Amazonia depend on deep root systems to maintain green canopies during the dry season. Evergreen forests in northeastern Pará state maintain evapotranspiration during five-month dry periods by absorbing water from the soil to depths of more than 8 m. In contrast, although the degraded pastures of this region also contain deep-rooted woody plants, most pasture plants substantially reduce their leaf canopy in response to seasonal drought, thus reducing dry-season evapotranspiration and increasing potential subsurface runoff relative to the forests they replace. Deep roots that extract water also provide carbon to the soil. The forest soil below 1 m depth contains more carbon than does above-ground biomass, and as much as 15% of this deep-soil carbon turns over on annual or decadal timescales. Thus, forest alteration that affects depth distributions of carbon inputs from roots may also affect net carbon storage in the soil.

Pastures are the most common type of vegetation on deforested land in Amazonia. They vary greatly in the ratio of grass to woody-plant cover, including managed pastures (from which woody vegetation is removed by heavy machinery) and the more common shrub- and tree-dominated "degraded" pastures[15–17]. We studied deep roots in a mature, evergreen forest and in adjacent pastures near the town of Paragominas, in the Brazilian state of Pará. The deeply weathered clay soils at the

‡ Present address: Department of Environmental Studies, Duke University, Durham, North Carolina 27708, USA.